Acta Medica et Biologica
Vol. 45, No. 4, 143-151, 1997

PCNA Index and Nuclear Morphometry for Diagnosing Higher Malignancies of Endocrine Cell Tumors in the Large Intestine

Ken NISHIKURA[1], Hidenobu WATANABE[1] and Mitsuya IWAFUCHI[2]

[1]First Department of Pathology, Niigata University School of Medicine, [2]Department of Medical Technology, College of Biomedical Technology of Niigata University, Niigata, Japan

Received June 19 1997; accepted September 8 1997

Summary. **Background: Endocrine cell tumors of the gastrointestinal tract are divided into the carinoid tumor (CD), a low-grade malignancy, and endocrine cell carcinoma (ECC), a high-grade malignancy. In this study, nuclear morphometry and proliferating cell nuclear antigen (PCNA) immunohistochemistry were performed to distinguish objectively between CDs and metastasizing CDs or ECCs.**

Methods: Nuclear morphometry and PCNA immunohistochemistry were performed on the following colorectal endocrine cell tumors: 15 primary CDs and 1 metastatic focus, 5 primary ECCs and 3 metastatic foci, and their counterparts of 5 solid adenocarcinomas and 3 metastatic lesions. To differentiate the tumors from one another and to elucidate which features are responsible for metastasis in CDs.

Results: Nuclear morphometric values (area, circumference, and short diameter) significantly increased in the order of CDs, ECCs, and adenocarcinomas, and were positively correlated with the PCNA index (PI) and particularly with a PI of strongly positive cells (PI-S). The PI and PI-S significantly increased in the order of CDs, ECCs, and adenocarcinomas ($p<0.01$). A 20.0×17.0 mm CD, which extended down into the muscle layer metastasized to the lymph nodes and liver, contained a high-grade atypical (HGA) area. The HGA area, 10.6 mm^2 located in the submucosa, showed nuclear morphometric values quite similar to those of a nodal metastatic lesion, and its PI and PI-S were significantly higher than in the remaining primary CD area, but lower than in ECCs.

Conclusions: Nuclear morphometry and PCNA index are useful for distinguishing CDs from more malignant CDs or ECCs, and for detecting the progressive potentiality of CDs.

Correspondence: Ken Nishikura, First Department of Pathology, Niigata University School of Medicine, Asahimachi-dori 1, Niigata 951, Japan.

Key words—endocrine cell tumor, carcinoid tumor, endocrine cell carcinoma, large intestine, PCNA, nuclear morphometry.

INTRODUCTION

Histologically and biologically, endocrine cell tumors of the gastrointestinal tract are divided into two groups:[1] the carcinoid tumor (CD), a low-grade malignancy, and endocrine cell carcinoma (ECC) synonymous with small cell carcinoma, a high-grade malignancy. CDs are characterized by trabecular, ribbon-like or solid structures composed of uniform small cells with rare mitotic figures, whereas ECCs are generally characterized by solid structures comprised of cells larger than those of CDs, as well as many mitotic figures, a high nucleocytoplasmic ratio, and large atypical nuclei.[2-6] Some carcinoid tumors metastasize to the lymph nodes or liver. However, there are few reports that distinguish CDs from metastasizing CDs or ECCs by nuclear morphometry and cellular proliferative activity. While there are four reports regarding the proliferative activity of gastrointestinal endocrine cell tumors,[7-10] three of these papers do not clarify whether the endocrine cell tumors in their materials belong to CDs or ECCs, and none makes detailed mention of the correlation between proliferative activity and size, depth of invasion, histological pattern of the tumors.

The purpose of the current study is to analyze nuclear morphometric differences between CDs and more malignant CDs or ECCs of the large intestine, and to evaluate the correlation between the morphometric findings and proliferative activity by im-

munohistochemistry, using a monclonal antibody to proliferating cell nuclear antigen (PCNA).

MATERIALS AND METHODS

In this study, endocrine cell tumors are those tumors that grow in specific histological patterns, such as trabecular, ribbon-like, and/or solid, and that consist of round to ovoid cells with diffuse positivity for at least one of the already known endocrine cell markers such as Grimelius' argyrophil stain, chromogranin A, neuron-specific enolase, or the endocrine-granule constituent.

For morphometric and immunohistochemical analysis, 15 rectal CDs, 5 ECCs (2 rectal, and 3 colonic), and 5 solid adenocarcinomas (1 rectal, and 4 colonic) were selected from the cases registered in the First Department of pathology, Niigata University School of Medicine, from 1982 to 1994. All tumors were endoscopically or surgically resected from Japanese patients without systemic adjuvant therapy. Twenty-four patients had a single tumor and one had an independent tumor of CD and ECC.

In this study, all of the primary tumors and their seven metastatic tumors (one from CD, three from ECCs and three from adenocarcinomas) were available for analysis (Table 1). As controls, solid areas of adenocarcinomas, except for tubular formation or mucous production, were picked up. All of the tumors were fixed in 10% formalin solution immediately after resection, cut into 2- to 4-mm-thick pieces along the largest diameter of each tumor within 1 to 11 days after resection (4.4 days on the average), and then embedded in paraffin. Each of the serially cut sections from one or two representative blocks, 2-μm thick, was stained with hematoxylin-eosin (HE) stain; victoria-blue stain for elastic fibers; Factor-VIII stain for endothelial cells of vascular channels; Grimelius' argyrophil stain, chromogranin A, neuron-specific enolase, and endocrine-granule constituent for endocrine cell markers; and PCNA stain.

In CDs and ECCs, cell clusters longer than 50 μm were divided into two histological patterns: trabecular (cord-like or ribbon-like clusters) and solid (sheet-like or nodular clusters), in order to study the correlation of their patterns with morphometric values and the PCNA index (PI).

Immunohistochemical procedure for PCNA stain

Air-dried paraffin sections were deparaffinized with xylene and dehydrated with ethanol. Then they were stained for PCNA with a streptavidin-biotin immunoperoxidase (SAB) method using a Histofine SAB- PO kit (Nichirei Co., Tokyo, Japan). The sections were immersed for 30 min with 0.3% H_2O_2 in methanol, quenched of endogenous peroxidase activity, and then treated with 10% normal rabbit serum for blocking nonspecific immunoreaction. The sections were then incubated with mouse monoclonal anti-PCNA antibody PC10 (Novo Castra Laboratories, Newcastle, UK), diluted 1 : 200 in phosphate-buffered saline, for 30 min at room temperature. Then they were incubated with biotinylated rabbit antimouse immunoglobulin for 20 min and subsequently with streptavidin-peroxidase for 30 min at room temperature. After these treatments, the sections were carefully visualized with 3 : 3′-diaminobenzidine tetrachloride (DAB). The reaction times in the DAB solution, which were decided section by section under the direct observation of each proliferative zone of the non-neoplastic mucosa in order to cope with various formalin fixation times, ranged between 0.5 and 2.2 min. Lastly, the sections were counterstained faintly with hematoxylin.

Evaluation of PCNA stain

A brown-colored nucleus confirmed at ×400 magnification, regardless of granular or homogeneously nongranular reaction, was judged as PCNA-positive. Staining intensity was semiquantitatively classified into two patterns: weak (+; positive nuclei were light brown at higher magnification), and strong (++; positive nuclei were deep brown). The distribution and index of proliferative cells in non-neoplastic colorectal crypts were used as inner positive controls for the PCNA stain in each section.

PCNA index (PI) and PI of strongly positive cells (PI-S)

The PI and PI of strongly positive cells (PI-S) were expressed as the percentage of PCNA-positive cells to the total number of tumor cells examined in an area (average 1121 cells; range 970 to 1964), picked up from tumor tissues as being histologically homogeneous in cellular atypia and mitotic frequency. PI and PI-S were measured on: 32 submucosal (sm) areas of 13-sm CDs; 6 sm areas and 6 muscularis propria (mp) areas of 2 mp-invading CDs; 18 sm areas, and 19 mp and further invading areas of 5 ECCs; 6 sm areas, and 18 mp and further invading areas of 5 solid adenocarcinomas (Table 1). Tumor tissues with dense inflammatory or necrotic changes were excluded from this evaluation.

PI and PI-S were estimated separately to elucidate

their correlation with nuclear morphometric values, sm-area size, depth of invasion, metastasis, and histological pattern (trabecular vs solid).

Nuclear morphometry

The morphometry was done in each area corresponding to that in which PI was counted. Its parameters included: nuclear area (A), nuclear circumference (C), and short diameter of the nucleus (SD). Using a computerized image analyzing system (Image Command 5098: Olympus Optical Co., Tokyo, Japan) at a magnification of ×220 (×40 objective and ×5.5 eyepiece), an average of 106 cells (range 100 to 125) per area were measured.

The morphometry for CDs was done separately on 13 sm-invading CDs and 2 mp-invading CDs, as the former showed neither vessel permeation nor metastasis, though the latter disclosed venous permeation in one case and, in the other, lymphatic permeation, a histologically confirmed nodal metastasis, and a macroscopic metastatic nodule extending into the liver (Table 1).

Mitotic index (MI)

Mitotic figures were confirmed by PCNA staining. MI was expressed as a ratio of mitotic cells to 1,000

Table 1. Examined cases of endocrine cell tumors

Cases		Fixation time (day)	Location of tumor	Depth of invasion	Largest diameter (mm)	Largest sm area (mm^2)	Vascular permeation		Distant metastasis	
							v	ly	n	others
CD	1	4	R	sm	3.5	5.8	0	0	−	−
	2	1	R	sm	6.0	11.8	0	0	−	−
	3	2	R	sm	6.0	13.3	0	0	−	−
	4	1	R	sm	6.0	14.9	0	0	−	−
	5	4	R	sm	6.5	17.1	0	0	−	−
	6	1	R	sm	7.0	21.8	0	0	−	−
	7	4	R	sm	8.0	23.2	0	0	−	−
	8	10	R	sm	8.0	23.6	0	0	−	−
	9	1	R	sm	8.5	24.9	0	0	−	−
	10	1	R	sm	8.5	29.5	0	0	−	−
	11	1	R	sm	8.0	32.5	0	0	−	−
	12	2	R	sm	8.9	38.3	0	0	−	−
	13	1	R	sm	11.0	54.0	0	0	−	−
	14	1	R	mp	13.0	87.2	1	0	−	−
	*15	6	R	mp	20.0	95.0	0	1	+	liver
ECC	1	3	R	mp	30.0		1	1	−	−
	*2	8	A	mp	55.0		1	2	+	−
	3	4	R	mp	80.0		1	0	−	−
	*4	6	C	ss	62.0		1	3	+	−
	*5	11	A	si	150.0		1	2	−	kidney
Adn	*1	10	A	ss	45.0		1	1	+	−
	*2	6	A	ss	40.0		1	1	+	−
	*3	3	A	se	70.0		0	3	+	−
	4	5	R	al	70.0		1	3	−	−
	5	8	C	se	130.0		3	1	−	−

CD, carcinoid; ECC, endocrine cell carcinoma; Adn, solid adenocarcinoma; R, rectum; A, ascending colon; C, caecum; n, lymph node; sm, submucosa; mp, muscularis propria; ss, subserosa; se, serosa; si, serosa and infiltrating other organs; al, adventitia

Number in vascular permeation. 0, no permeation; 1, 2, and 3, mild, moderate, and severe permeation, respectively.

*Metastatic tumor was also available for morphometry and immunohistochemistry.

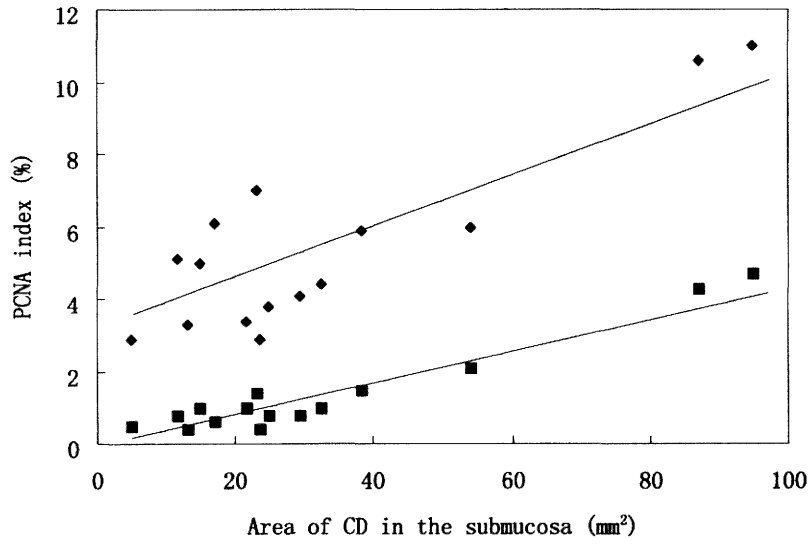

Fig. 1. Correlation of PCNA index to the submucosal area of CD.

tumor cells in the same area as that used to determine the PI and PI-S snd in the corresponding area to that of the morphometry.

Statistical analysis

Statistical analysis of the difference was estimated using the *t*-test or chisquare test. A statistically significant difference was presumed when the *p*-value was less than 0.05.

RESULTS

Nuclear morphometry

(1) CDs

The average nuclear morphometric values in submucosal areas of 13 sm-invading CDs were 35.6±6.1 (average±standard deviation) μm^2 in area (A), 23.2±2.1 μm in circumference (C), and 5.6±0.7 μm in short diameter (SD) (Table 2 and Fig. 2A). In the 2 mp-invading CDs excluding the HGA area (as described below), there was no significant difference in the nuclear morphometric values between the sm layer and the mp layer (sm vs mp; A: 40.4±8.0 vs 39.8±7.1; C: 24.8±3.0 vs 24.5±3.2; SD: 5.8±0.7 vs 5.7±0.7). In the contrast, the values were significantly larger in the sm foci of the 2 mp-invading CDs than in those of the sm-invading CDs ($p<0.01$) (Table 2).

The metastasizing case had a 10.6 mm^2 sm-tumor area (11.2% of the total 95.0 mm^2 sm-tumor area) composed of HGA cells with a high nucleocytoplasmic ratio, and large and irregular shaped nuclei (Fig. 3A). The HGA area showed significantly higher values for the three parameters of nuclear morphometry than the sm-invading CDs (Table 2). The metastatic focus of one lymph node also revealed HGA cells closely related in nuclear morphometric findings to those of the HGA area (Table 2 and Fig. 3C). The HGA area, both in the primary and metastatic sites, showed nuclear morphometric values similar to those of the primary and metastatic ECCs. However, as compared with ECC, the HGA area showed lower cellular density, and the component cells had more finely dispersed chromatin and a more abundant, clearer cytoplasm, indicating a lower nucleocytoplasmic ratio (Fig. 3A).

There was no significant difference in morphometric values between the trabecular pattern of the 15 primary CD cases and the solid pattern of the 4 cases excluding the HGA area (trabecular vs solid; A: 36.4±6.6 vs 35.9±6.8; C: 23.5±2.3 vs 22.9±2.3; SD: 5.7±0.7 vs 5.6±0.7).

Table 2. Nuclear morphometry of endocrine cell tumors and adenocarcinomas

Tumor	Part examined (No. of areas and cells)		Nuclear morphometry		
			Area (m^2)	Circumference (μm)	Short diameter (μm)
CD	sm-CD	(32) (3448)	#35.6±6.1	#23.2±2.1	#5.6±0.7
	sm part of mp-CD	(6) (659)	40.4±8.0#	24.8±3.0#	5.8±0.7#
	HGA area	(1) (112)	#51.9±14.3	#28.1±4.0	#6.9±1.1
	Metastasis	(1) (108)	51.8±11.1	27.4±3.0	7.1±1.0
ECC	Primary				
	meta (−)	(15) (1587)	45.8±10.5#	26.1±3.5#	6.4±1.4#
	meta (+)	(22) (2314)	46.5±11.9	26.2±3.4	6.5±1.7
	Metastasis	(4) (419)	46.9±12.4	26.4±3.8	6.5±1.3
Adeno-carcinoma	Primary				
	meta (−)	(10) (1031)	63.5±11.9	31.5±4.0	7.4±1.2
	mesa (+)	(14) (1486)	63.8±13.0	31.5±4.4	7.5±1.1
	Metastasis	(5) (531)	64.1±12.1	31.7±4.5	7.5±1.4

HGA area, high-grade atypical area; #$p<0.01$ (t-test).

Table 3. Mitotic index and PCNA index of endocrine cell tumors and adenocarcinomas

Tumor	Part examined (No. of areas and cells)		Mitotic index (%)	PCNA index (%)	PCNA index of strong positivity (%)
CD	sm-CD	(32) (40179)	#0.1±0.1	#4.5±1.4	#0.9±0.5
	sm part of mp-CD	(6) (7638)	1.2±0.7#	10.1±1.3#	4.6±0.5#
	HGA area	(1) (1498)	#2.3±0.2	#16.0±2.1	#8.4±2.0
	Metastasis	(1) (1964)	3.1±1.0	19.8±1.0	10.1±0.1
ECC	Primary				
	meta (−)	(15) (16677)	#7.1±2.0	#48.8±18.6	#31.8±10.7
	meta (+)	(22) (20832)	7.6±2.1#	49.5±14.8#	32.9± 9.4#
	Metastasis	(4) (3952)	11.7±3.3	67.7± 8.8	45.7± 9.1
Adeno-carcinoma	Primary				
	meta (−)	(10) (9264)	#13.2±4.0	#70.8±4.8	#55.8±6.8
	meta (+)	(14) (13800)	13.8±4.1#	71.5±4.9#	56.9±6.9#
	Metastasis	(5) (5859)	15.3±1.3	78.9±5.1	63.9±7.4

HGA area, high-grade atypical area; #$p<0.01$ (χ^2-test).

(2) ECCs

ECCs showed significantly larger nuclear morphometric values than CDs within the three parameters ($p<0.01$) (Table 2 and Fig. 4A). However, among ECCs, no significant difference was found in the values between the sm layer and the deeper layers (sm vs deeper layers; A: 45.7±13.1 vs 46.6±12.4; C: 26.1±4.1 vs 26.2±4.1; SD: 6.4±1.2 vs 6.4±1.0), or between the solid pattern of five cases and the trabecular of two cases (solid vs trabecular; A: 45.6± 11.0 vs 46.8±12.9; C: 26.1±3.3 vs 26.4±3.9; SD: 6.4±

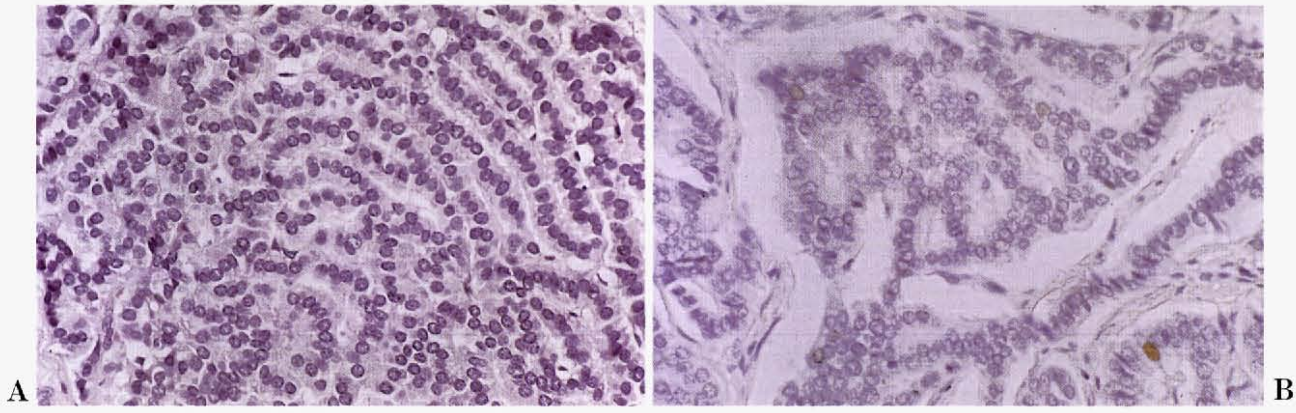

Fig. 2. **A.** A sm-invading carcinoid tumor (CD) showing a trabecular pattern composed of small cells without mitotic figures (HE stain, 2.5×40.0, Case CD-6), **B.** A few cells are positive for PCNA stain (PCNA stain, 2.5×40.0, Case CD-6).

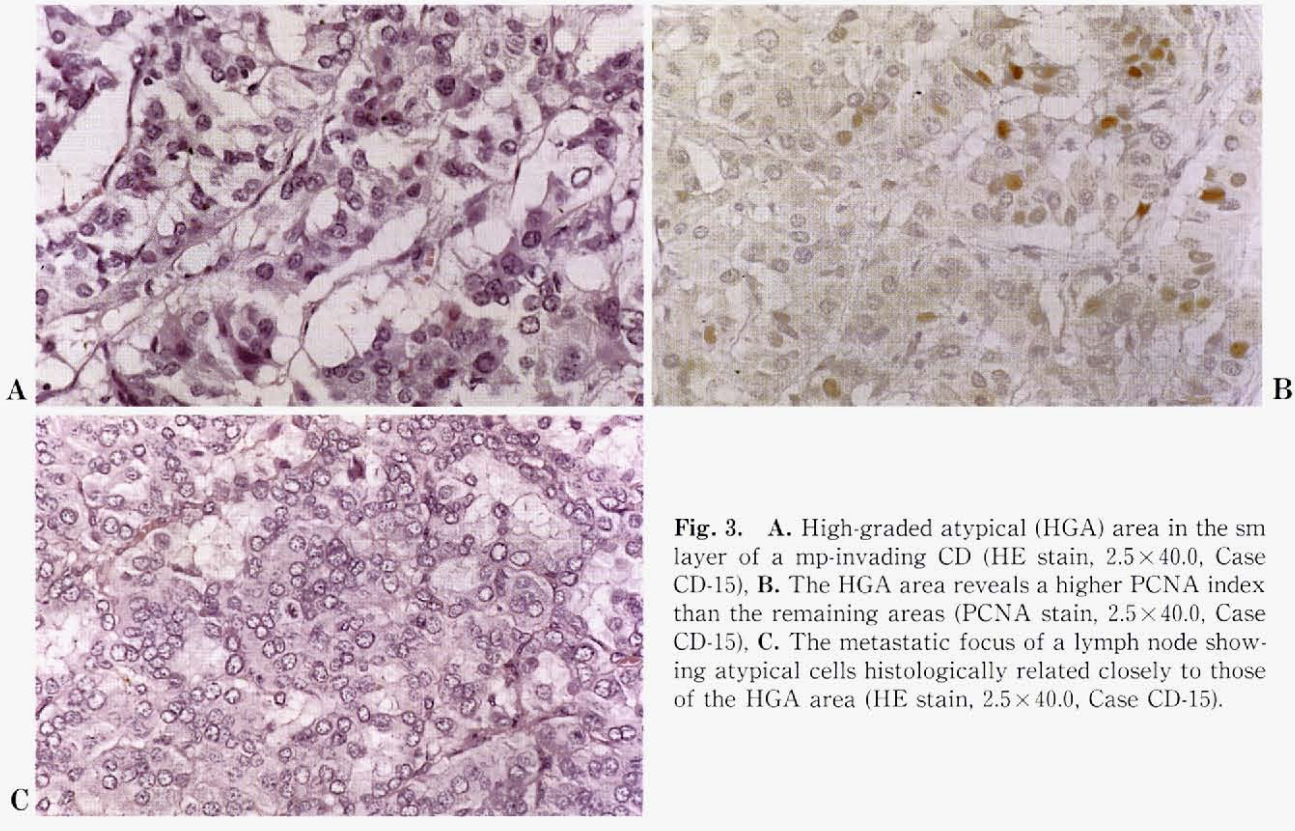

Fig. 3. **A.** High-graded atypical (HGA) area in the sm layer of a mp-invading CD (HE stain, 2.5×40.0, Case CD-15), **B.** The HGA area reveals a higher PCNA index than the remaining areas (PCNA stain, 2.5×40.0, Case CD-15), **C.** The metastatic focus of a lymph node showing atypical cells histologically related closely to those of the HGA area (HE stain, 2.5×40.0, Case CD-15).

1.5 vs 6.5±1.2).

The morphometric values did not differ in the primary site between three metastatic and two non-metastatic cases, or between three primary tumors and their metastatic tumors (Table 2).

(3) Solid adenocarcinomas

Five solid adenocarcinomas showed significantly larger nuclear morphometric values than did the CDs or ECCs ($p<0.01$) (Table 2). The morphometric values

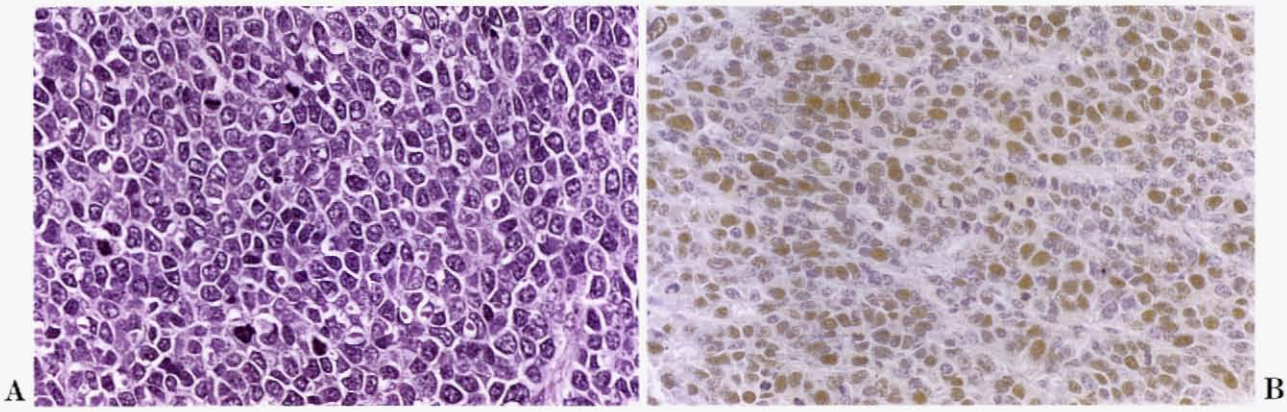

Fig. 4. **A.** An endocrine cell carcinoma (ECC) case consists of atypical cells with a solid pattern and frequent mitotic figures (HE stain, 2.5×40.0, Case ECC-4), **B.** Diffuse distribution of PCNA-positive cells (PCNA stain, 2.5×40.0, Case ECC-4).

of solid adenocarcinomas did not differ between the sm layer and the deeper layers (sm vs deeper layers; A: 63.6±8.3 vs 63.7±14.1; C: 31.5±4.0 vs 31.6±4.1; SD: 7.4±1.2 vs 7.4±1.2), between three metastatic and two nonmetastatic tumors, and between three primary tumors and their metastatic tumors (Table 2).

MI, PI, and PI-S

(1) Inner positive controls

PI and PI-S of the proliferative zone cells in non-neoplastic crypts in each tumor section revealed no significant difference among CDs, ECCs, and solid adenocarcinomas regardless of formalin-fixation time: the PI and PI-S were, on an average; 1) 53.4±1.8 and 24.9±0.4 in 4 cases fixed for one day, 2) 53.5±3.2 and 25.2±1.9 in 14 cases fixed from 2 to 4 days, and 3) 54.1±3.5 and 25.3±2.1 in 7 cases fixed from 5 to 11 days (53.9±3.4 and 25.1±2.1 as average in total cases). MI also did not differ among cases.

(2) CDs

PCNA-positive cells were distributed homogeneously in each tumor regardless of the depth of invasion (Fig. 2B). In two mp-invading CDs excluding the HGA area, there was no significant difference in MI, PI, and PI-S between the sm layer and the mp layer (sm vs mp; MI: 1.2±0.7 vs 1.1±0.2; PI: 10.1±1.3 vs 10.0±1.4; PI-S: 4.6±0.5 vs 4.5±0.3). The sm foci of mp-invading CDs, however, revealed significantly higher MI, PI, and PI-S than those of sm-invading CDs (Table 3). No significant difference was found between the trabecular pattern and the solid, excluding the HGA area (trabecular vs solid; MI: 0.5±0.6 vs 0.4±0.6; PI: 6.0±2.9 vs 5.8±2.7; PI-S: 2.5±0.5 vs 2.2±0.3).

On the other hand, the HGA area of a primary CD indicated significantly higher MI, PI, and PI-S than the remaining areas, and lower indices than a nodal metastatic focus (Table 3 and Fig. 3B).

The PI and PI-S correlated well with the size of the submucosal area of 15 primary CDs excluding the HGA area (PI: $r=0.864$, $p<0.01$; PI-S: $r=0.963$, $p<0.01$) (Fig. 1).

(3) ECCs

PCNA-positive cells were diffusely distributed in all five tumors (Fig. 4B). ECCs, both in the primary and metastatic sites, indicated significantly higher MI, PI, and PI-S than CDs ($p<0.01$) (Table 3). The indices did not differ significantly between the sm layer and deeper layers (sm vs deeper laters; MI: 7.3±2.1 vs 7.5±2.2; PI: 48.7±15.0 vs 49.4±14.6; PI-S: 31.7±9.8 vs 32.8±8.8), between the solid pattern and the trabecular (solid vs trabecular; MI: 7.2±1.1 vs 7.5±1.0; PI: 48.2±4.1 vs 49.2±2.7; PI-S: 31.4±3.6 vs 32.6±3.4), or between three primary tumors with metastasis and two primary tumors without metastasis (Table 3). However, the metastatic foci showed significantly higher MI, PI, and PI-S than did the primary tumors ($p<0.01$) (Table 3), in spite of no significant difference in nuclear morphometric values (Table 2).

(4) Solid adenocarcinomas

PCNA- positive cells were diffusely distributed in the observed solid areas of all five adenocarcinomas, which revealed significantly higher MI, PI, and PI-S than CDs and ECCs ($p<0.01$) (Table 3). No significant

difference was found in the indices between the sm layer and the deeper layers of the five carcinomas (sm vs deeper layers; MI: 13.6±3.8 vs 13.4±4.1; PI: 71.9±10.8 vs 71.0±11.7; PI-S: 57.0±16.7 vs 56.2±17.1), or between three primary tumors with metastasis and two primary tumors without metastasis, but a significant difference was found between primary tumors and metastatic foci ($p<0.01$) (Table 3), regardless of the lack of significant difference in nuclear morphometric values (Table 2).

Relationship among MI, PI, PI-S, and nuclear morphometric values

PI and PI-S of CDs, ECCs, and adenocarcinomas correlated well with one another ($r=0.98$), and with MI (PI: $r=0.97$; PI-S: $r=0.99$). The PI and PI-S also showed a significant correlation with each of the morphometric parameters (PI and PI-S; A: $r=0.66$ and 0.71; C: $r=0.68$ and 0.71; SD: $r=0.64$ and 0.69).

DISCUSSION

Histological differentiation of CDs from ECCs has been described through findings of hematoxylin-eosin (HE)-stained sections in the WHO Blue Book (2nd-edited)[1] and others,[2,6] but not by more objective methods such as morphometry or PCNA immunostaining. For the first time, this study confirmed a significant difference in nuclear morphometric values between CDs and ECCs, and between CDs and more malignant CDs (CDs with high-grade atypia). In addition to the morphometric analysis, we performed PCNA immunohistochemistry to compare the proliferative activity with morphometric values in endocrine cell tumors.

The morphometric values significantly differentiated sm-CDs from ECCs. Furthermore, MI, PI, and PI-S were more clearly distinguished between them; that is, ECCs indicated significantly higher MI, PI, and PI-S than sm-CDs and mp-CDs. In addition, the nuclear morphometric values of CDs and ECCs positively correlated with PI, particularly with PI-S. The difference of proliferative activities between CDs and ECCs suggests that the latter grows much faster than the former. The high proliferative activity of ECCs may reflect, in part, their aggressive biological behavior. Kimura et al.[10] analyzed 42 neuroendocrine cell tumors including 28 gastrointestinal tract CDs and one gastric ECC, and reported that the average PCNA index was 26.8% in CDs and 92.1% in ECCs, findings much higher than our data. However, their paper contains no precise descriptions on depth of invasion and size of tumors investigated, reaction time for immunostaining, and PCNA index of inner positive controls.

A 20.0×17.0 mm mp-CD contained an HGA area in the sm layer. The HGA area showed significantly higher morphometric values than sm-CDs, and significantly higher MI, PI, and PI-S than sm-CDs and the remaining areas of the mp-CDs. The HGA area was considered to be a transformation from low-grade to high-grade malignancy caused by a progression of tumor cells with a subsequent increase in tumor size. Further, the HGA area seemed to play an important role in metastasis, because its nuclear morphometric values were closely related to those of a nodal metastatic lesion. However, the HGA area showed a lower cellular density and lower nucleocytoplasmic ratio than in ECCs. Furthermore, MI, PI, and PI-S of the HGA area were lower than those of ECCs. It is generally considered to be rare for ECCs to develop from CDs through malignant transformation.[6] The HGA area, therefore, should be included in CDs rather than in ECCs, and it is biologically more reasonable that a CD is cytologically divided into a CD with low grade atypia and a CD with high grade atypia.

In general, CDs more than 20 mm in diameter are considered to have malignant potential. Soga[11] evaluated 1097 reported cases of gastroenteropancreatic carcinoid tumors (no detailed histological descriptions) and reported that the frequency of distant metastasis was respectively 4.8% (22/522) of the tumors less than 11 mm, 29.7% (66/222) of the 11 to 20 mm, 52.1% (111/213) of the 21 to 50 mm, and 66.5% (93/140) of the more than 50 mm. Ishikawa et al.[12] reported on 42 rectal carcinoid tumors (no detailed histological descriptions) in which mp-invasion was seen in none of 22 tumors less than 10 mm, 11.8% (2/17) of 10 to 19 mm tumors and 66.7% (2/3) of the more than 19 mm. In our current study, mp-CDs disclosed venous permeation in one case (13 mm in size), and lymphatic permeation and metastases to the lymph node and liver in another case (20 mm in size), whereas none of 13 sm-CDs 11.0 mm or less in diameter (54.0 mm^2 or less in the sm area), showed vessel permeation or metastasis. Our data provide histological explanations concerning the increasing ability of vascular permeation and/or mp-invasion of the more than 11.0 mm CD and on distant metastasis of the more than 20.0 mm CD.

In primary CDs, each PI and PI-S was positively correlated with the size of the submucosal area of the tumors. The sm part of mp-invading CDs indicated significantly higher PI and PI-S than sm-invading CDs. Our data suggest that populations of prolifer-

ative cells are responsible for tumor growth and invasive ability.

The half-life time of the PCNA protein is about 20 h; it may be detectable in cells that have recently left the cell cycle.[13,14,15] Hall et al.[15] reported the presence of weak PCNA-positive cells out of the proliferative zone in the gastrointestinal tract. They also described the increased expression of PCNA in non-neoplastic condition adjacent to the tumors. Wolf et al.[16] reported that prolonged fixation in formalin caused a loss of numbers of PCNA-positive cells, especially with a weak stain. These reports suggest the variable immunoreactivity of PCNA, especially when the PCNA reaction products are weak in color. In this study staining intensity of PCNA was semiquantitatively graded as weak and strong, and the PCNA index was respectively evaluated as PI (index of all positive cells) and PI-S (index of strongly positive cells). Both the PI and PI-S of each inner control showed no significant differences according to the fixation time. Furthermore, PI and PI-S correlated well with one another ($r=0.98$), and both revealed a significant correlation with each of the morphometric values.

We conclude that PCNA immunohistochemistry is greatly useful not only for distinguishing CD from ECC, but also for detecting a higher malignancy in CD that is devoid of obvious histological changes.

REFERENCES

1) Watanabe H, Jass JR, Sobin LH: Histological typing of oesophageal and gastric tumors, 2nd ed. Berlin, Springer-Verlag, 1990, p 19-28.
2) Matsusaka T, Watanabe H, Enjoji M: Oat-cell carcinoma of the stomach. *Fukuoka Acta Med* **67:** 65-73, 1976.
3) Iwafuchi M, Shibuki S, Watanabe H: An endocrine cell carcinoma with coexisting adenocarcinoma and extramammary Paget's disease in the rectum. *J Jpn Soc Coloproc* **35:** 51, 1982. (in Japanese)
4) Iwafuchi M, Ishihara N, Watanabe H: Histogenesis of endocrine cell carcinoma of the stomach. *Jpn J Cancer Clin* **30:** 435-437, 1984. (in Japanese)
5) Iwafuchi M, Watanabe H, Noda Y, Ajioka Y, Enjoji M, Itoh M: Gastrointestinal carcinoid tumors of Japanese: Incidence and characteristics based on anatomical classification, with special reference to difference between carcinoid tumor and endocrine cell carcinoma. *Stomach and Intestine* **24:** 869-882, 1989. (in Japanese)
6) Iwafuchi M, Watanabe H, Ishihara N, Noda Y, Ajioka Y: Carcinoid tumor and endocrine cell carcinoma of the gastrointestinal tract: their characteristics and histogenesis. *Clin Gastroenterol* **5:** 1669-1681, 1990. (in Japanese)
7) Chaudhry A, Oberg K, Wilander E: A study of biological behavior based on the expression of a proliferating antigen in neuroendocrine tumors of the digestive system. *Tumor Biol* **13:** 27-35, 1992.
8) Herbay A, Sieg B, Schurmann G, Hofmann WJ, Betzler M, Otto HF: Proliferative activity of neuroendocrine tumors of the gastoenteropancreatic endocrine system: DNA flow cytometric and immunohistological investigation. *Gut* **32:** 949-953, 1991.
9) Hayashi H, Nakagawa M, Kitagawa S, Yamada T, Ishida K, Kurumaya H: Immunohistochemical analysis of gastrointestinal carcinoids. *Gastroenterol Jpn* **28:** 483-490, 1993.
10) Kimura N, Nagura H: A comparative study of neuroendocrine carcinoma and carcinoid tumor with special reference to expression of HLA-DR antigen and PCNA. *Zentralbl-Pathol* **139:** 171-175, 1993.
11) Soga J: Statistical analysis of carcinoid tumors. *Clin Gastroenterol* **5:** 1661-1667, 1990. (in Japanese)
12) Ishikawa T, Ushio K, Kusaka K, Sekiguchi R, Mizuguchi Y, Nawano S: The diagnosis and treatment of rectal carcinoid. *Stomach and Intestine* **24(8):** 891-902, 1989. (in Japanese)
13) Bravo R, Celis JE: A search for differential polypeptide synthesis throughout the cell cycle of HeLa cells. *J Cell Biol* **84:** 795-802, 1980.
14) Bravo R, Macdonald-Bravo H: Existence of two populations of cyclin/proliferating cell nuclear antigen during the cell cycle: Association with DNA replication sites. *J Cell Biol* **105:** 1549-1554, 1987.
15) Hall PA, Levison DA, Woods AL, Yu CC-W, Kellock DB, Watkins JA, Barnes DM, Gillett CE, Camplejohn R, Dover R, Waseem NH, Lane DP: Proliferating cell nuclear antigen (PCNA) immunolocalization in paraffin sections: An index of cell proliferation with evidence of deregulated expression in some neoplasms. *J Pathol* **162:** 285-294, 1990.
16) Wolf HK, Dittrich KL: Detection of proliferating cell nuclear antigen in diagnostic histopathology. *J Histochem Cytochem* **40:** 1269-1273, 1992.